NeuroImage 45 (2009) 453–462

Contents lists available at ScienceDirect

NeuroImage

journal homepage: www.elsevier.com/locate/ynimg

Forward and backward connections in the brain: A DCM study of functional asymmetries

C.C. Chen [a,*], R.N. Henson [b], K.E. Stephan [a,c], J.M. Kilner [a], K.J. Friston [a]

[a] Wellcome Trust Centre for Neuroimaging, Institute of Neurology, University College London, 12 Queen Square, London, WC1N 3BG, UK
[b] MRC Cognition & Brain Sciences Unit, Cambridge, UK
[c] Laboratory for Social and Neural Systems Research, Institute for Empirical Research in Economics, University of Zurich, Switzerland

ARTICLE INFO

Article history:
Received 15 October 2008
Revised 16 December 2008
Accepted 17 December 2008
Available online 31 December 2008

Keywords:
Nonlinear coupling
Neuronal dynamics
Induced responses
Dynamic causal modelling
Spectral responses
Backward connection
Recurrent connection
Reentrant dynamics
Predictive coding

ABSTRACT

In this paper, we provide evidence for functional asymmetries in forward and backward connections that define hierarchical architectures in the brain. We exploit the fact that modulatory or nonlinear influences of one neuronal system on another (*i.e.*, effective connectivity) entail coupling between different frequencies. Functional asymmetry in forward and backward connections was addressed by comparing dynamic causal models of MEG responses induced by visual processing of normal and scrambled faces. We compared models with and without nonlinear (between-frequency) coupling in both forward and backward connections. Bayesian model comparison indicated that the best model had nonlinear forward and backward connections. Using the best model we then quantified frequency-specific causal influences mediating observed spectral responses. We found a striking asymmetry between forward and backward connections; in which high (gamma) frequencies in higher cortical areas suppressed low (alpha) frequencies in lower areas. This suppression was significantly greater than the homologous coupling in the forward connections. Furthermore, exactly the asymmetry was observed when we examined face-selective coupling (i.e., coupling under faces minus scrambled faces). These results highlight the importance of nonlinear coupling among brain regions and point to a functional asymmetry between forward and backward connections in the human brain that is consistent with anatomical and physiological evidence from animal studies. This asymmetry is also consistent with functional architectures implied by theories of perceptual inference in the brain, based on hierarchical generative models.

Introduction

This paper is about functional asymmetries between forward and backward connections in the brain. Dynamic causal modelling (DCM), a recently developed modelling framework, was used to ask if there is an asymmetry in nonlinear or modulatory influences among different levels of a cortical hierarchy. We addressed this asymmetry using MEG data obtained from human subjects during the processing of faces and tried to explain the observed responses using models that do and do not have nonlinear connections. This enabled us to quantify the evidence for nonlinear coupling in qualitative terms, using model comparison. We then compared forward and backward coupling strengths quantitatively, to test for any asymmetries, under the best model.

Hierarchical connections and functional asymmetries

It is now generally accepted that, at least in the sensory cortex, the brain has a hierarchical organisation that is defined largely by asymmetries in extrinsic cortico-cortical connections (Maunsell and van Essen, 1983; Zeki and Shipp, 1988; Felleman and Van Essen, 1991; for motor systems this issue is more controversial, see Shipp, 2005). These asymmetries classify a connection as being forward or backward (Rockland and Pandya, 1979) and therefore define an implicit (although not necessarily unique; Hilgetag et al., 2000) hierarchy of areas. The laminar specificity of forward and backward projections is a key anatomical asymmetry, which may speak to ensuing functional asymmetries (Sandell and Schiller, 1982; Murphy and Sillito, 1987; Salin and Bullier, 1995; Lamme et al., 1998; Angelucci et al., 2002a,b). One of the important aspects of this anatomical asymmetry is that backward connections make synaptic connections predominantly in supra-granular layers, with en-passant connections in infra-granular layers. This is relevant because voltage sensitive (*i.e.*, nonlinear) receptors like NMDA receptors populate, largely, the supra-granular layers (Fox et al., 1989; Rosier et al., 1993), suggesting that backward connections may have preferential access to modulatory, voltage-dependent post-synaptic effects with long time-constants (*c.f.*, Eaton and Salt, 1996; Gentet and Ulrich, 2004). Similarly, backward connections have also been found to target metabotropic glutamate receptors which, like NMDA receptors, have long time-constants and are thus able to mediate context-sensitive effects (Rivadulla et al., 2002; Salt, 2002). The notion that backward connections are more

* Corresponding author. Fax: +44 207 813 1445.
E-mail address: c.chen@fil.ion.ucl.ac.uk (C.C. Chen).

1053-8119/$ – see front matter © 2008 Elsevier Inc. All rights reserved.
doi:10.1016/j.neuroimage.2008.12.041

modulatory, in relation to the driving effects of forward connections (Salin and Bullier, 1995; Sherman and Guillery, 1998), is further supported by the higher degree of divergence that backward connections display and by their ability to transcend more than one cortical level (Zeki and Shipp, 1988). In short, most of the evidence from the anatomy of extrinsic (inter-regional) connections, from the spatial distribution of their synaptic connections across cortical layers and from their physiology, points to a functional asymmetry between forward and backward connections. This asymmetry is consistent with a role for backward connections in modulating, coordinating or providing contextual guidance to bottom-up processing that is driven by forward connections. There are many examples of this ranging from the mediation of extra-classical receptive field effects (Angelucci and Bressloff, 2006; Hupe et al., 1998; Lamme and Roelfsema, 2000) to the implementation of gain mechanisms that may be involved in attention and biased competition (Larkum et al., 2004). Indeed, direct evidence for the modulatory effect of backward connections has been obtained from reversible deactivation studies in monkeys (Sandell and Schiller, 1982; Girard and Bullier, 1989; Hupe et al., 1998) and non-invasive fMRI studies of humans (Friston et al., 1995; Büchel and Friston, 1997; Stephan et al., 2008). However, there have been no direct comparisons of modulatory effects in forward and backward connections in man.

Modulatory effects and nonlinear coupling

The defining characteristics of modulatory pre-synaptic inputs are nonlinear interactions with other pre-synaptic inputs when generating post-synaptic responses. Examples here include the mechanisms of classical neuromodulatory neurotransmitters that, for example, change the conductance of slow potassium channels that mediate after hyper-polarisation (*e.g.*, Metherate et al., 1992; Faber and Sah, 2003). These sorts of effects change the response profile of neurons, such that they respond differently to the same driving input. Another key example is the voltage-dependence of NMDA receptor activation, which means that the effect of pre-synaptically released glutamate at these receptors is context-sensitive and nonlinear (e.g., Schiller and Schiller, 2001). A third important example of nonlinear interactions relates to action potentials that are back-propagated by means of active conductances throughout the dendritic tree to elicit long-lasting calcium currents; this means that, depending on the relative timing of synaptic inputs, the propagation of postsynaptic potentials can be facilitated or blocked by preceding synaptic inputs (*e.g.*, Larkum et al., 2004; London and Häusser, 2005).

The equivalence between modulatory effects of synaptic connections and nonlinearities in neuronal input-output relations is important because nonlinear effects can be characterised relatively easily using only the observable inputs and outputs of a system. In brief, nonlinear effects induce high-order generalised convolution kernels, in the time domain, or generalised transfer functions in the spectral domain (Friston, 2001). These high-order functions couple certain frequencies in the input to *different* frequencies in the output. A simple example here would be the nonlinear squaring of a sinusoidal wave to double its frequency. This means we can formulate questions about the modulatory effects in terms of coupling between frequencies in spectral responses that are observed in different parts of the brain. This is the basis of a recently developed dynamic causal model (Friston et al., 2003) for EEG and MEG (Chen et al., 2008) that allows one to test various models with and without nonlinear (between-frequency) coupling among specified regions or sources. The current report is based on this approach.

Nonlinear coupling and generative models in the brain

There are many heuristics that have been used to frame the importance of nonlinear or modulatory coupling in the brain. We focus on a specific but dominant account of functional anatomy, based on hierarchical inference and learning in the brain (Helmholtz, 1860; MacKay, 1956; Ballard et al., 1983; Mumford, 1992; Kawato et al., 1993; Dayan et al., 1995; Rao and Ballard, 1999; Rao, 1999; Friston, 2003; Kersten et al., 2004; Friston, 2005; Friston et al., 2006). This account suggests that the brain is an inference machine that uses generative models to predict incoming sensory information. In this framework, also referred to as predictive coding (Rao and Ballard, 1999; Friston, 2005), perceptual inference corresponds to optimising putative causes of sensory input by minimising prediction error (or, equivalently, variational free-energy). This can be achieved simply by generating predictions at higher levels of the cortical hierarchy, which are passed to lower levels to explain away bottom-up inputs. These predictions are updated by prediction errors, conveyed by the forward connections. This scheme entails forward and backward message passing and is formally identical to hierarchical or empirical Bayesian inference (Friston, 2003). Critically, because predictions are formed using a generative model of the world, this account predicts that the influence of backward connections is necessarily nonlinear (Friston, 2003). A simple example of nonlinearity, in generative models of visual input, would be the occlusion of one object by another. If higher level representations of an object and its occluder are used to provide a prediction of the sensory input, then these top-down effects must interact nonlinearly to encode the occlusion *per se*. In short, under empirical Bayesian or predictive coding models of perceptual inference, backward connections that convey predictions that should suppress activity in lower levels encoding prediction error. Critically, this explaining away of prediction error rests on nonlinear mechanisms. This is compatible with the physiological evidence, described above, that backward connections mediate modulatory effects.

The functional properties of forward connections are predominantly, but not exclusively, linear; see Friston, 2003 and Sherman and Guillery, 1998 for a summary of the neurophysiological evidence. However, there is some empirical evidence that forward connections may also exhibit nonlinear properties. For example, transmission of sensory information along forward connections can involve NMDA receptors (Fox et al., 1990; Kelly and Zhang, 2002; Salt, 2002). According to predictive coding theories, forward connections mediate the influence of error units in lower levels on representational units in higher levels, and these bottom-up influences are linear in prediction error (Friston, 2003). However, "… although the forward connections mediate linearly separable effects, these connections might be activity- and time-dependent because of their dependence on [higher representations]" Friston (2003). This means the strengths of forward connections may be activity-dependent and therefore appear nonlinear.

In summary, on the basis of the above empirical and theoretical considerations we predicted that coupling between high and low areas would entail cross-frequency or nonlinear coupling. This is because there is substantial evidence that at least one arc (backward connections) of reciprocal self-organising exchanges between visual areas rests on nonlinear synaptic mechanisms. Furthermore, we predicted that backward coupling would suppress neuronal activity in lowers areas and that this suppression would; (i) be manifest as a significant cross-frequency (nonlinear) suppression (ii) be significantly greater than the equivalent coupling in the forward direction. To test these hypotheses, we used a recently validated dynamic causal model for induced responses measured with M/EEG (Chen et al., 2008) to implement different models with and without nonlinear (between-frequency) coupling among regions involved in visual face processing. Using Bayesian model selection (Penny et al., 2004), we compared models in which forward and backward connections could either be linear or nonlinear. We were hoping to show that, qualitatively, nonlinear models were significantly better than their linear homologues. We then examined the coupling estimates from the best model to test the quantitative hypotheses about the suppressive effects of backward connections.

This paper comprises three sections. In the first, we briefly summarise dynamic causal modelling for induced responses. This technique is then applied to an MEG study of face perception, as described in the second section. This section describes the factorial construction of four DCMs that were inverted to provide the evidence for each model and subject (*i.e.*, probability of the data given the model). We then identified the best model using Bayesian model comparison and established the consistency of model selection at the between-subject level by analysing the model evidences. In the final section, we present the quantitative characterization of coupling using the conditional parameters estimated of the best model to test for predicted top-down suppression and forward-backward asymmetries.

Dynamic causal modelling for induced responses

Dynamic causal modelling (Friston et al., 2003) uses a dynamic or state-space model to explain observed time-series. Because these models are formulated in terms of differential equations and account for experimentally controlled perturbations or inputs they can be regarded as causal in nature; hence dynamic causal modelling. Usually a dynamic causal model has two components; the first comprises a set of differential equations describing the causal evolution of hidden states of the system generating data. Second, an observer function maps the hidden states to observed responses. These equations form the basis of a likelihood model, which together with a prior constitute a probabilistic generative or forward model. This model can then be inverted, given observed data using established variational techniques (*i.e.*, Friston et al., 2007).

Dynamic causal modelling is now well established for functional magnetic resonance (fMRI) time series (e.g. Bitan et al., 2005; Ethofer et al., 2006; Fairhall and Ishai, 2007; Fan et al., 2007; Grol et al., 2007; Mechelli et al., 2003; Stephan et al., 2007a) and has recently been applied to electromagnetic data as observed with EEG and MEG (Garrido et al., 2007; Kiebel et al., 2008; David et al., 2007) or invasively recorded local field potentials (Moran et al., 2008). Even more recently, we have described a dynamic causal model for spectral responses as summarised by time-frequency representations of source-reconstructed EEG or MEG data (Chen et al., 2008). In brief, DCM for induced responses involves three steps: model specification, feature selection and model inversion. Model specification entails specifying a number of sources generating the observed channel data, the sparsity structure of connections among these sources and whether the connections are nonlinear or not. Feature selection involves computing the time-dependent expression of different frequencies at each source. This is simple to do because the forward model, given the sources, is over-determined and can be inverted easily to give the time-series $x_i(t)$ at each source. A time-frequency analysis of source-specific activities then provides the time-dependent spectral activity over a range of frequencies at the i-th source[1].

$$\tilde{g}_i(\omega,t) = \begin{bmatrix} \tilde{g}(\omega_1,t) \\ \vdots \\ \tilde{g}(\omega_K,t) \end{bmatrix}$$
$$\tilde{g}(\omega_k,t) = \left|\int x_i(s-t)\exp\left(-j\omega_k s - s^2/2\sigma^2\right)ds\right|^2 \quad (1)$$

where ω denotes frequency, t represents time and s indexes time within a moving Gaussian window of width σ. The likelihood model of these spectral features is very simple; it is based upon a linear approximation to the state-equations describing the evolution of frequency-specific power at one source as a function of power in all other sources and frequencies. A bilinear form for the state equations allows one to model the modulation of connectivity by experimental manipulations (*i.e.* faces *vs.* scrambled faces in this study).

$$\tau\dot{g}(\omega,t) = \tau\begin{bmatrix}\dot{g}_1 \\ \vdots \\ \dot{g}_J\end{bmatrix} = \left\{\begin{bmatrix}A_{11} & \cdots & A_{1J} \\ \vdots & \ddots & \vdots \\ A_{J1} & \cdots & A_{JJ}\end{bmatrix} + X\begin{bmatrix}B_{11} & \cdots & B_{1J} \\ \vdots & \ddots & \vdots \\ B_{J1} & \cdots & B_{JJ}\end{bmatrix}\right\} g(\omega,t) + \begin{bmatrix}C_1 \\ \vdots \\ C_J\end{bmatrix} u(t) \quad (2)$$

Here, the matrices A and C contain coupling parameters that control, respectively, changes in spectral activity due to endogenous coupling with other sources and changes induced by exogenous (*e.g.*, stimulus) inputs, $u(t)$. The matrices B represent the modulation of the endogenous coupling parameters in A by an experimental manipulation encoded by $X \in \{1,0\}$ for two conditions (e.g., faces and scrambled faces). The coupling matrices are composed of blocks:

$$A_{ij} = \begin{bmatrix} a_{ij}^{11} & \cdots & a_{ij}^{1K} \\ \vdots & \ddots & \vdots \\ a_{ij}^{K1} & \cdots & a_{ij}^{KK} \end{bmatrix} \quad B_{ij} = \begin{bmatrix} b_{ij}^{11} & \cdots & b_{ij}^{1K} \\ \vdots & \ddots & \vdots \\ b_{ij}^{K1} & \cdots & b_{ij}^{KK} \end{bmatrix} \quad C_i = \begin{bmatrix} c_i^1 \\ \vdots \\ c_i^K \end{bmatrix} \quad (3)$$

where the elements a_{ij}^{kl} encodes how changes in the k-th frequency in the i-th source depend on the l-th frequency in the j-th source and b_{ij}^{kl} represents the corresponding change in coupling that is induced experimentally. The leading diagonal elements of the A matrices are minus one; this means that each frequency has an intrinsic tendency to decay or dissipate. Similarly, c_i^k controls the frequency-specific influence of exogenous inputs on the k-th frequency in the i-th source. This enables within and between-frequency coupling within and between sources. See Fig. 1 for a schematic summary of the model.

The coupling parameters define the effective connectivity between sources and frequencies, while priors on these parameters define the particular model in terms of which sources and frequencies are coupled. Linear connections between two sources are encoded by parameters coupling the same frequency in both sources, whereas nonlinear connections are represented by parameters coupling different frequencies. By changing the priors, one can switch these parameters on or off (for details, see Chen. et al. 2008). Specifically, one can construct different models that do or do not allow for nonlinear coupling between different sources. The advantage of the bilinear form in Eq. (3) is that we can restrict the experimental effect to a subset of connections and compare the ensuing models. We will use this to model face-selective effects in, and only in, forward and backward extrinsic connections.

Predictions of the observed spectral responses are formed by perturbing the system with a parameterised (gamma function) input over all frequencies and integrating the predicted response over peristimulus time. Under Gaussian assumptions about observation error, $\varepsilon(\omega,t)$, this provides a likelihood model for observed data, which can be inverted using standard techniques as described in Friston et al. (2007).

$$\tilde{g}(\omega,t) = g(\omega,t) + \varepsilon(\omega,t). \quad (4)$$

The results of inversion comprise a free-energy bound on the log-evidence of the model $\ln p(\tilde{g}|m)$ and the conditional density of its parameters $p(A,B,C|\tilde{g},m)$. When several models are inverted, inference on model-space proceeds by comparing the log-evidences $\ln p(\tilde{g}|m_i)$ for each model, as described below. After the best model has been identified, inference on its parameters proceeds using their conditional estimates. In the context of multi-subject studies the evidence is pooled by simply adding the log-evidences over subjects (because the data from each subject are conditionally independent).

Inference on coupling parameters

Typically, dynamic causal models are applied to time-series data from single-subjects or sessions. Characterising the model parameters

[1] We use $\tilde{g}(\omega,t)$ for the observed spectral features and $g(\omega,t)$ for the true but hidden values.

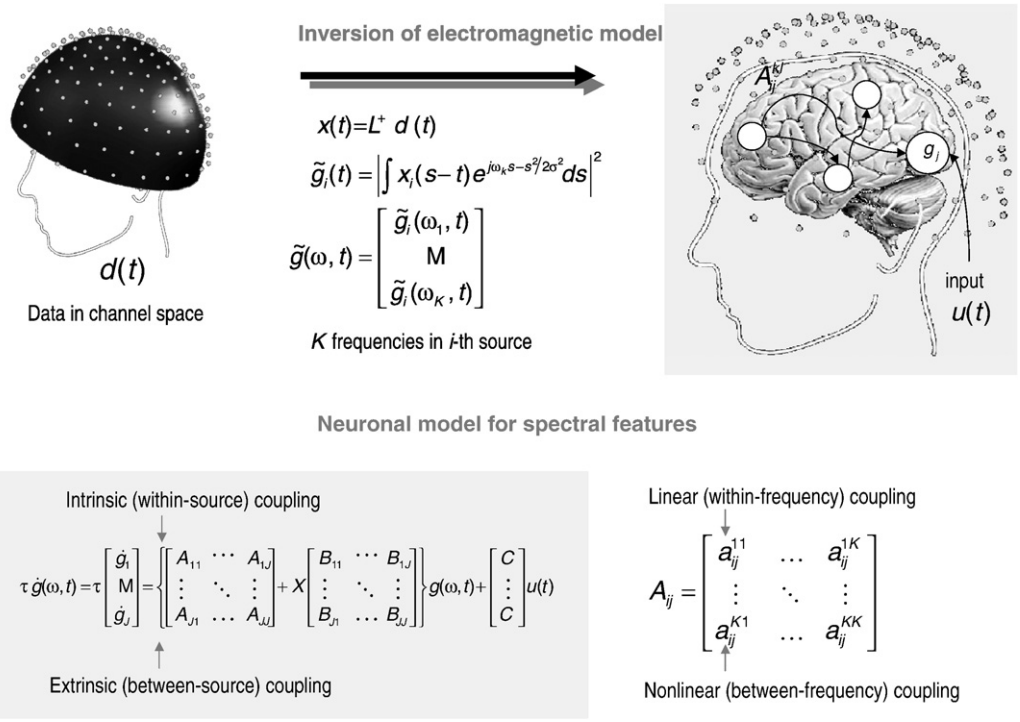

Fig. 1. Schematic illustration of DCM for induced responses. Upper panel: The spectral dynamics in the sources, $\tilde{g}_i(t)$, are first evaluated from observations in sensor space and projected onto source space using the pseudo-inverse of the lead-field, $L \in \Re^{sxc}$; for s sources and c channels. The spectral densities obtain by squaring the absolute values after a Morlet wavelet transform. Lower panel: the bilinear form of state equations. At the source level, the DCM comprises a vector of states for each electromagnetic source, allowing for linear and nonlinear coupling.

over subjects usually uses a summary statistic approach, in which the conditional estimates are passed to a second (between-subject) level for classical inference. This is the procedure we pursue here, with an interesting difference: in DCM for induced responses, each connection is characterised by a matrix or field of coupling parameters, $A_{ij}(\omega_k,\omega_l)=a_{ij}^{kl}$, that link all frequencies in the source to all frequencies in the target. Under narrow-band linear coupling, all the elements of this coupling matrix will lie along the leading diagonal, because one frequency in the source can only affect the same frequency in the target. With nonlinear coupling the coupling matrix has large off-diagonal entries, whereby a high or a low frequency in the source can change a low or high frequency in the target. Critically, at the between-subject level, we have to deal with coupling matrices, as opposed to single connection strengths. We do this using conventional statistical parametric mapping that properly accommodates smoothness or dependencies among the elements of the coupling matrices, when controlling false positive rates (Kilner et al. 2005). The results of these analyses are statistical parametric maps (SPMs) that show significant differences in coupling among different frequencies, for each connection or mixtures of connections.

Data acquisition and analysis

Experimental design and data pre-processing

We analysed spectral responses induced by face processing in ten normal subjects as measured with MEG (Henson et al., 2007). Here, we analyse data from a single, eleven minute session, in which subjects saw intact or scrambled faces, subtending visual angles of approximately four degrees. We chose these data because visual processing of face stimuli *vs*. degraded face stimuli is an example of a perceptual process that has been investigated previously and interpreted in terms of predictive coding principles (*c.f.* Summerfield et al., 2006). Scrambled versions of each face were created by phase-shuffling in Fourier space and masking by the outline of the original image. The scrambled faces were therefore matched for spatial frequency power density and size. Subjects made left-right symmetry judgments about each stimulus by pressing one of two keys with either their left or right index finger (range of reaction times was 1031 to 1798 ms). There were 86 intact and 86 scrambled face artefact-free trials as revealed by visual inspection. Ten subjects were tested, five female (young to middle-aged adults). The MEG data were sampled at 625 Hz on a 151-channel axial gradiometer CTF Omega system at the Wellcome Trust Laboratory for MEG Studies, Aston University, England. No subject moved more than 6 mm across the session (median = 1.1 mm, range = 0.2–5.6 mm).

The MEG data were pre-processed using SPM5 (Wellcome Trust Centre for Neuroimaging, London). The data were epoched from −600 to +1800 ms, and projected from channel space to source-space using the generalised inverse of the lead-field matrix for our chosen sources (see Model specification below for details). The lead-field (gain matrix) was computed using the coregistered channel locations and a single-sphere forward model computed by Fieldtrip (F.C. Donders Centre for Cognitive Neuroimaging, Nijmegen, as implemented in SPM5). The spectral densities from 4 to 48 Hz at each source were computed using a time-frequency Morlet wavelet transform (Eq. (1); wavelet number: 7) between −100 and 600 ms of peristimulus time. The resulting time-frequency responses were first converted to absolute values and averaged over 86 trials for each condition and then baseline-corrected by subtracting the frequency-specific power of the first time-bin. For computational expediency, we reduced the dimensionality of spectra to four principal frequency components derived from a singular value decomposition (SVD) of the spectra (over conditions and peristimulus time, within subjects). This preserved over 93 % of the spectral variance in all subjects. Note that the generalised inverse of the lead-field described here is one of many inversion schemes that one can use to project data from channel to source space (Darvas et al., 2004; Friston et al., 2008; Kiebel et al.,

2008; Michel et al., 2004). The generalised inverse is an appropriate projector if one knows *a priori* where the sources are located. However, the results of any model inversion under these prior assumptions are conditional on the chosen sources being a reasonable summary of the real neuronal sources. If any sources are omitted and misplaced there will be a better model of the data and possibly a different conclusion from model comparison. If one did not know where the spectral signals were coming from, the beam-former method could be one useful strategy that allows one to localize the source positions and estimate spectral features empirically (Singh et al 2003).

Model specification

The anatomical source locations were the maxima of ventral temporal activations in a group SPM analysis of fMRI data from exactly the same paradigm though different subjects (Henson et al. 2003). Those sources have also been reported in MEG face studies (Henson et al. 2007; Itier et al., 2006). Fig. 2 shows the location of these sources in Montreal Neurological Institute (MNI) coordinates and on a template MRI image in that space (Talairach and Tournoux, 1988). These four sources correspond to the fusiform face area (FFA) and the occipital face area (OFA), bilaterally. The central panel of Fig. 2 shows the connectivity graph, which served as the basis for constructing alternative DCMs. We assumed reciprocal intra-hemispheric connections between OFA and FFA and reciprocal inter-hemispheric connections between homotopic areas. Additionally, we assumed cross-hemispheric connections between OFA and contralateral FFA. This connection was added because a previous fMRI study of a prosopagnosic patient with lesions of left FFA and right OFA found normal activation in the right FFA for faces *vs.* non-faces (Rossion et al. 2003). One possible input to this patient's right FFA is from the intact contralateral OFA. We therefore included forward connections from OFA to contralateral FFA. The connectivity architecture for the models considered in this study is shown in Fig. 3. All models included reciprocal connections between the visual and fusiform areas within and across the hemispheres. Stimuli entered the left and right OFA. We used a factorial approach to specify our models, which systematically varied the form of the *A* and *B* matrices in Eq. 2: Our models differed according to whether the forward and backward connections, (and implicitly their modulation by face-selective processing) were linear or nonlinear (see upper left panel in Fig. 3). This resulted in four models (lower panel in Fig. 3):

F_LB_L: linear forward connections and linear backward connections.
F_NB_L: nonlinear forward connections and linear backward connections.
F_LB_N: linear forward connections and nonlinear backward connections.
F_NB_N: nonlinear forward connections and nonlinear backward connections.

We restricted face-selective effects (encoded by the B matrix) to intra-hemispheric forward and backward connections. Clearly, these models are a highly simplified representation of the "core system" for face processing identified by Haxby and colleagues (Haxby et al., 2000; Fairhall and Ishai, 2007). However, they are sufficient to address our question, *i.e.* to distinguish between linear and nonlinear coupling in a hierarchical neuronal network.

Bayesian model comparison and statistical testing

We compared alternative models in terms of their log-evidence. For any given pair of models, this difference is the equivalent, in log-space, to computing their so-called Bayes factor, *i.e.* their evidence or marginal likelihood ratio (Penny et al. 2004). A difference of three or more (i.e. a Bayes factor of about twenty) is usually considered as "strong" evidence in favour of one model relative to another (Penny et al. 2004). To ensure differences in the summed log-evidences were consistent over subjects, the log-evidences for each subject and model were entered into a one-way, repeated-measures analysis of variance (ANOVA).

To make inferences about the coupling parameters of the best model, the conditional expectations of the forward and backward coupling matrices were entered into a conventional between-subject SPM analysis to identify significant, frequency-specific, differences in effective connectivity. We tested for significant negative or suppressive effects in backward connections, relative to forward connections for coupling under face processing (*A* plus *B* matrices). We then repeated this comparison for the face-selective component of coupling (*B* matrix). After performing these *t*-tests we computed an SPM of the *F*-statistic to ensure that our planned comparisons had not

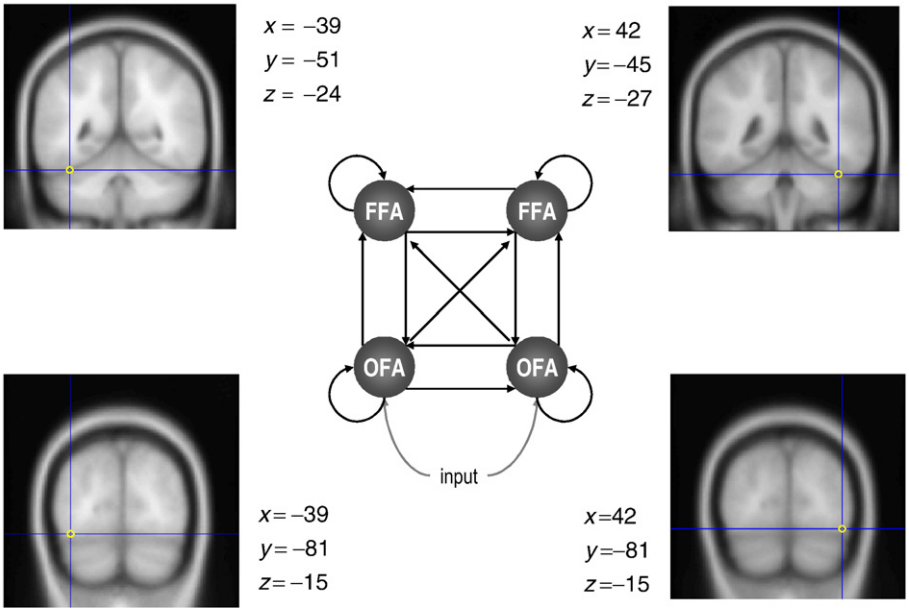

Fig. 2. Location of the four sources (in MNI coordinates) shown on a template MRI image. The central panel shows the basic connectivity structure of the models, which are presented in more detail in Fig. 3. *OFA*: left and right occipital face area; *FFA*: left and right fusiform face area.

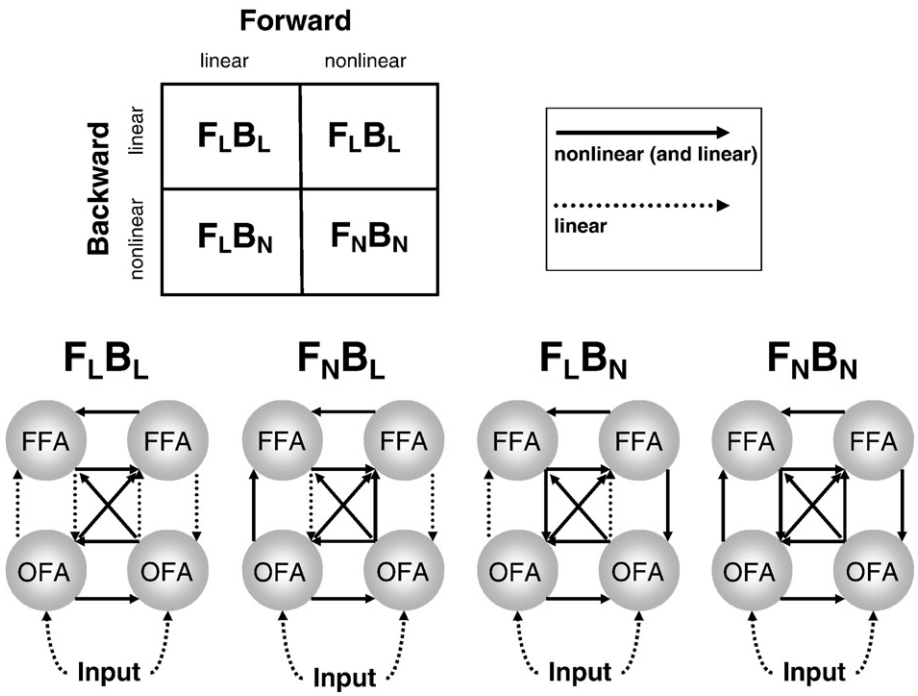

Fig. 3. The upper panel shows the factorial structure of model space: models differed according to whether the forward and backward connections (and implicitly their modulation by face vs. scrambled face stimuli) were linear or nonlinear. The lower panel shows the connectivity architecture of the ensuing DCMs. The solid and dashed lines indicate nonlinear and linear connections, respectively. N: nonlinear coupling; L: linear coupling; F: forward connection; B: backward connection. For simplicity, the intrinsic (self) connections are omitted. These were nonlinear (see previous figure).

missed any other significant differences. The SPM were displayed at $p<0.05$ (uncorrected) and we report maxima at a corrected $p<0.05$ level (Kilner et al. 2005).

Results

Inference on models

Four DCMs were inverted for each subject as described above. The summed log-evidences over subjects are shown in Fig. 4 (left panel). It can be seen that the best model is F_NB_N (log-evidence sum = −11895), followed by F_LB_N (−16306), F_NB_L (−16308) and F_LB_L (−59890). In other words, the model with nonlinear forward and backward connections was vastly superior to all other models, whereas the model with linear forward and backward connections was clearly the worst. The two 'mixed' models were fairly similar in log-evidence (*i.e.*, positive but not strong evidence for exclusive nonlinear coupling in backward connections relative to forward connections). A repeated-measures ANOVA showed there was a significant interaction ($F=13.468$; $p=0.005$; df 1.9); suggesting that when backward connections are linear, the log-evidence is greatly affected by whether forward connections are nonlinear; conversely, when backward connections are nonlinear, the log-evidence is much less influenced by the nature of forward connections (see Fig. 4; right panel). *Post-hoc* t-tests, confirmed that nonlinear model was significantly better than all other models (F_LB_L: $t=4.473$, $p=0.001$; F_NB_L: $t=1.908$, $p=0.044$; F_LB_N: $t=2.306$, $p=0.023$; $df=9$).

To verify that our assumptions about the basic connectivity structure (*c.f.* Fig. 2) were sound, we created two variants of the F_NB_N model. These included a simplified model (sF_NB_N) that contained no cross-hemispheric OFA–FFA connections and a more complex model (cF_NB_N) that contained reciprocal (as opposed to unidirectional) cross-

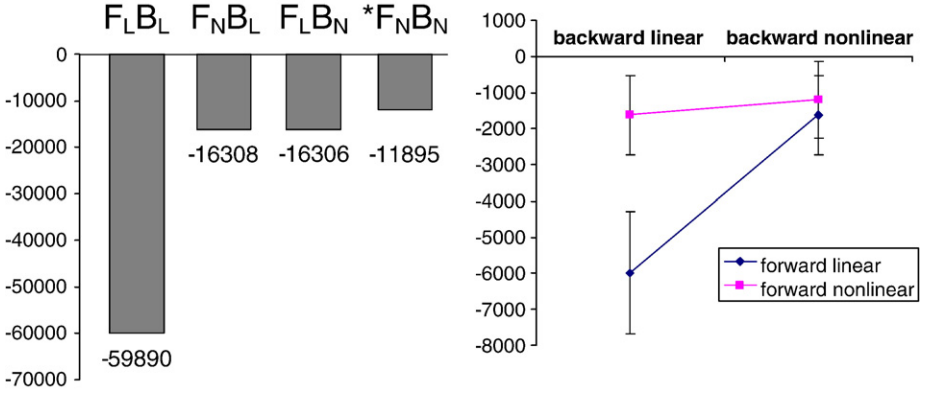

Fig. 4. *Left panel:* Summed log-evidences for the four DCMs, pooled over subjects. It can be seen that the best model is F_NB_N, followed by F_LB_N, F_NB_L and F_LB_L. *Right panel*: The averaged log-evidence for all four models with standard errors.

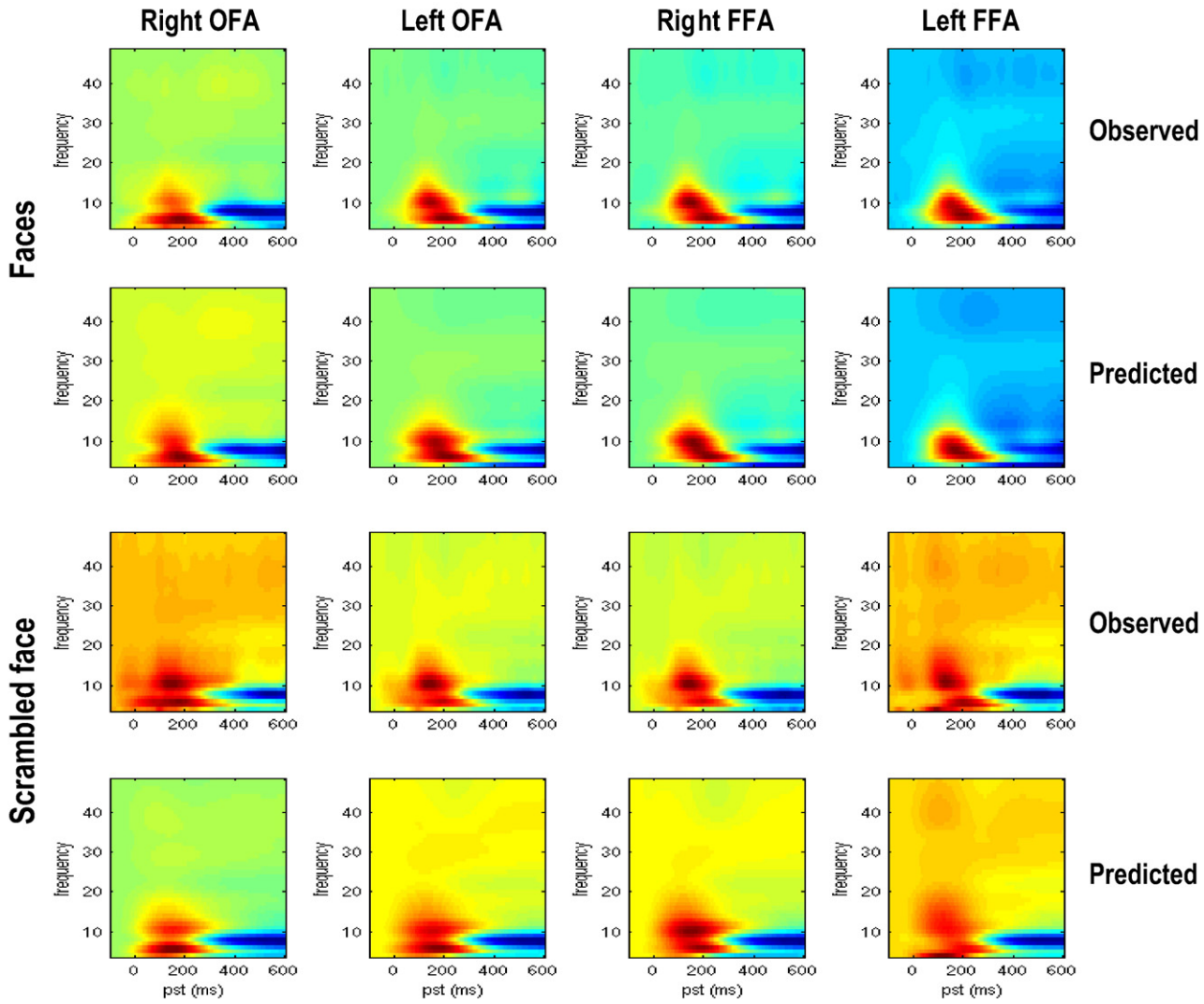

Fig. 5. This figure shows predicted and observed spectral responses for a representative subject, at the source level, under the best model (F_NB_N), for the two experimental conditions (faces *vs.* scrambled faces). The top two rows are the observed and predicted spectra for normal faces; the bottom two rows are the observed and predicted spectra for scrambled faces.

hemispheric OFA–FFA connections. Bayesian model comparison demonstrated that both were clearly inferior to the nonlinear model. Their summed log-evidences were −17243 (sF_NB_N) and −15638 (cF_NB_N) and paired *t*-tests showed a significant difference in favour of the F_NB_N model ($p<0.047$ and $p<0.008$, respectively). The lower log-evidence for the cF_NB_N model provides another interesting demonstration (*c.f.*, Grol et al. 2007; Stephan et al. 2007b), that increasing the complexity of a model does not necessarily improve it.

In conclusion, we found that the model with nonlinear forward and backward connections was the best model and that the model with nonlinear backward connections came second. Fig. 5 shows the predicted (under the nonlinear model) and observed spectral responses at the source level, for the two experimental conditions (faces vs. scrambled faces) in a representative subject.

Inference on coupling parameters

Fig. 6 shows the coupling matrices during face processing for the forward and backward connections in the right and left hemispheres under the nonlinear model. These are the sum of the *A* and *B* matrices in Eq. (2), averaged over all subjects). Anecdotally, it can be seen that the forward (upper row) and backward (lower row) connections show profound nonlinear coupling with substantial off-diagonal structure. Furthermore, there are systematic differences between the forward and backward coupling; with the backward coupling showing negative or suppressive cross-frequency effects. Quantitatively, these are most marked in the right hemisphere for low (alpha) to high (gamma), and from gamma to alpha in both hemispheres (red arrows). We tested for these putative asymmetries with planned comparisons.

The SPM testing for a significant suppression in backward, relative to forward connections is displayed by Fig. 7 (thresholded at $p<0.05$ uncorrected). These comparisons used a stimulus times hemisphere times forward vs. backward repeated measures ANOVA with restricted maximum likelihood estimates of non-sphericity among the errors. The smoothness of the underlying residual fields was 7.8×6.5 Hz resulting in about 32 resolution elements (*i.e.*, effective samples over the frequency x frequency search space of the SPM). This comparison averaged over hemispheres because we failed to detect a hemisphere times connection interaction. The most (and only) significant difference (red arrow) was in the coupling from high (gamma) frequencies to low (alpha) frequencies. This difference was extremely significant ($t=4.72$; $p=0.002$, corrected; $df=72$). The subject-specific estimates of coupling strength for this cross-frequency coupling are shown in the lower panels for both hemispheres. In the right hemisphere, this difference is due mainly

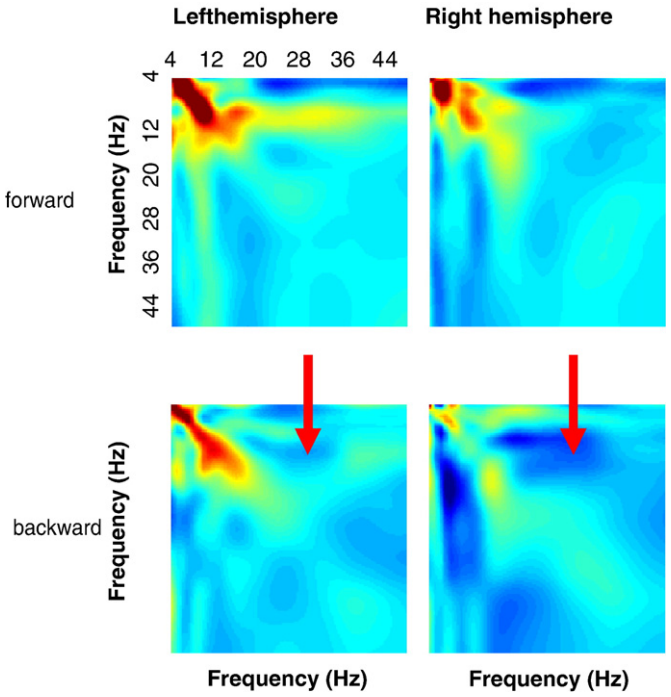

Fig. 6. Coupling matrices, averaged across subjects, for the coupling strengths of forward and backward connections in the right and left hemispheres of the $F_N B_N$ model.

to a suppressive effect of backward connections; where, remarkably, every subject had a negative connection strength. In the left hemisphere, the difference appeared to be augmented by an activating effect of forward connections.

We then repeated exactly the same analysis but testing for asymmetry in face-selective changes in coupling (*i.e.*, looking just at the *B* matrix). Although this comparison is not orthogonal to the previous comparison, it is reassuring to see that exactly the same differences. The only significant difference was again between gamma and alpha frequencies and was even more significant (t=5.09; p=0.001 corrected; df=72) than coupling under faces *per se* (Fig. 8; left panel). Finally, the right panel of Fig. 8 shows the SPM of the *F*-statistic testing for any differences in coupling over stimuli, hemispheres or connections. There were only three peaks that survived a corrected *p*-value of 0.05 and only one of these related to nonlinear coupling (F=5.78; p=0.006, corrected; df=8.72). This is exactly the same frequency-specific coupling identified by the planned comparisons. This SPM is shown to illustrate that the planned comparisons did not miss any other significant differences and shows that cross-frequency suppression mediated by backward connections, relative to forward connections, was the most prominent among all differences.

Discussion

Coupling between low and high frequency bands has been documented in both animal and human recordings (see Jensen and Colgin (2007) for a review). Canolty et al. (2006) demonstrated in humans that the power of high frequency gamma oscillations was modulated by the phase of the low-frequency theta rhythm. The implicit nonlinear coupling between oscillators at different frequencies builds upon previous studies that have identified similar phenomena in both anesthetised (Soltesz and Deschênes 1993) and behaving rats (Bragin et al. 1995). Here, we extend these observations by showing that nonlinear (between-frequency) interactions can be ascribed to specific intracerebral sources and used to disclose asymmetries in directed connections.

Intracranial EEG recordings have shown that faces elicit responses across a number of regions in the ventral temporal visual-processing pathway (Allison et al. 1994; Barbeau et al. 2008) and furthermore that faces can induce changes in the coherence of broadband (4–45 Hz) power between those regions (Klopp et al. 1999, 2000). However, little is known about the functional relevance of this coherence or, in particular, the role of nonlinear (between-frequency) coupling. It has been suggested that nonlinear coupling is a key aspect of functional integration and is an essential aspect of network function (Friston 2001; Jensen and Colgin, 2007; Tallon-Baudry and Bertrand, 1999; Varela et al. 2001). To our knowledge, this is the first study to quantify and make inferences about directed nonlinear coupling.

Model selection furnished strong evidence that nonlinear connections are important for explaining the current MEG data: indicating that the best model entailed nonlinearities in both forward and backward connections. The most marked difference in nonlinear coupling between forward and backward connections under this model was an activating effect of high (gamma) frequencies on low (alpha) frequencies in the forward connections and a suppressive effect in backward connections. Not only are these findings consistent with empirical evidence from invasive studies but confirmed theoretical predictions based on Bayesian treatments of perceptual inference. These predictions suggest that backward connections suppress or explain away prediction error as lower levels in cortical hierarchies using nonlinear synaptic mechanisms.

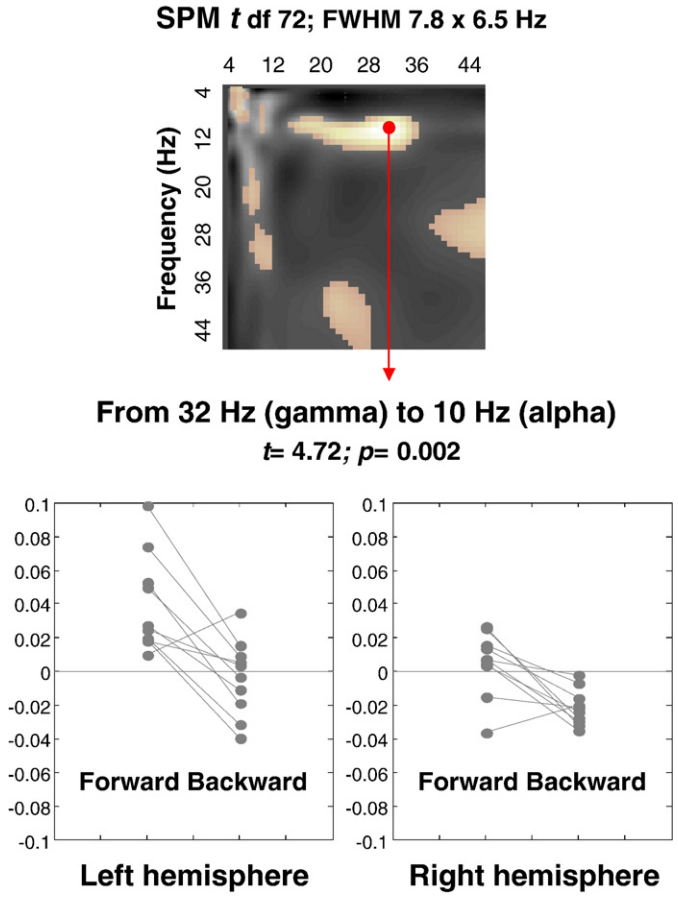

Fig. 7. *Upper panel*: SPM of the *t*-statistic testing for a greater suppressive effect of backward connections, relative to forward connections. The SPM is thresholded at $p<0.05$ (uncorrected). *Lower panels*: Subject-specific estimates of the coupling strength at the maximum of the SPM (red arrow) presented for each hemisphere.

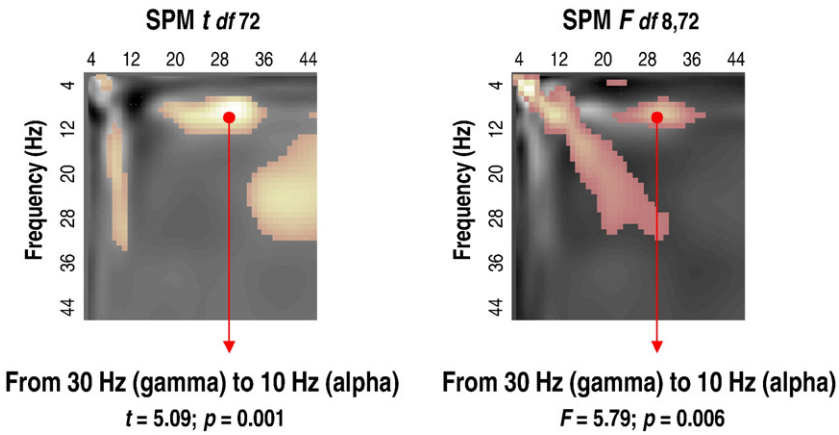

Fig. 8. *Left panel*: SPM of the *t*-statistic testing for a greater suppressive effect of backward connections, relative to forward connections in the face-selective changes coupling. *Right panel*: SPM of the *F*-statistic testing for any difference in frequency-specific coupling over connections, conditions or hemispheres. Both SPMs are thresholded at $p<0.05$ (uncorrected). Significant ($p<0.05$ corrected) peaks are indicated by the red arrows).

We were a bit surprised to find that high-frequencies affected low-frequencies. We had expected to see the converse given empirical results (*e.g.*, Canolty et al. 2006) and the simulations reported in Friston (2001). However, on reflection, the current results are entirely sensible if one considers that high (gamma) frequencies reflects increased neuronal firing (Chawla et al 1999): Heuristically, this means that gamma activity in low-level areas induces slower dynamics at higher cortical levels as prediction error is accumulated for perceptual synthesis. The concomitant high-level gamma activity (due to intrinsic nonlinear coupling) then accelerates the decay of evoked responses in the lower level that are manifest at, the population level, as damped alpha oscillations.

In conclusion, using a model-based approach that allows for probabilistic estimates of brain connectivity and its modulation by experimental conditions, our study provides empirical evidence for a functional asymmetry between forward and backward connections in the human brain that is consistent with neuroanatomical and neurophysiological data from animal studies. First, qualitative Bayesian model comparison disclosed overwhelming evidence for nonlinear models, in relation to formally equivalent models with linear coupling. Secondly, we found a striking quantitative asymmetry between forward and backward connections with regard to stimulus-bound and stimulus-specific (faces relative to scrambled faces) nonlinear coupling. This asymmetry was extremely significant and reproducible over subjects, even under the very conservative SPM procedures for multiple comparisons. This study is a starting point for further investigations of functional asymmetry between forward and backward connections in the human brain. Here, we restricted our models to the bilateral OFA and FFA regions believed to form the core of the visual face-processing system (Haxby et al., 2000). Future modelling studies will include other regions, such as posterior STS, which may also show changes in nonlinear coupling under other stimulus manipulations (e.g., different facial expressions, Winston et al. 2004).

Software note

All the analyses described in this paper can be performed using the SPM software available from http://www.filion.ucl.ac.uk/spm (erp api toolbox).

Acknowledgments

The Wellcome Trust funded this work. We are extremely grateful to Marcia Bennett for helping prepare this manuscript. C.C. Chen is funded by National Science Council of Taiwan (TMS-094-1-A-037), R.N. Henson is supported by the Medical Research Council (WBSE U.1055.05.012.00001.01), and K.E. Stephan is supported by the University Research Priority Program "Foundations of Social Human Behaviour" at the University of Zurich.

References

Allison, T., Ginter, H., McCarthy, G., Nobre, A.C., Puce, A., Luby, M., et al., 1994. Face recognition in human extrastriate cortex. J. Neurophysiol. 71, 821–825.
Angelucci, A., Bressloff, P.C., 2006. Contribution of feedforward, lateral and feedback connections to the classical receptive field center and extra-classical receptive field surround of primate V1 neurons. Prog. Brain Res. 154, 93–120.
Angelucci, A., Levitt, J.B., Walton, E.J., Hupe, J.M., Bullier, J., Lund, J.S., 2002a. Circuits for local and global signal integration in primary visual cortex. J. Neurosci. 22, 8633–8646.
Angelucci, A., Levitt, J.B., Lund, J.S., 2002b. Anatomical origins of the classical receptive field and modulatory surround field of single neurons in macaque visual cortical area V1. Prog. Brain Res. 136, 373–388.
Ballard, D.H., Hinton, G.E., Sejnowski, T.J., 1983. Parallel visual computation. Nature 306, 21–26.
Barbeau, E.J., Taylor, M.J., Regis, J., Marquis, P., Chauvel, P., Liegeois-Chauvel, C., 2008. Spatio temporal dynamics of face recognition. Cereb. Cortex 18, 997–1009.
Bragin, A., Jandó, G., Nádasdy, Z., Hetke, J., Wise, K., Buzsáki, G., 1995. Gamma (40–100 Hz) oscillation in the hippocampus of the behaving rat. J. Neurosci. 15 (1 Pt. 1), 47–60.
Büchel, C., Friston, K.J., 1997. Modulation of connectivity in visual pathways by attention: cortical interactions evaluated with structural equation modelling and fMRI. Cereb. Cortex 7, 768–778.
Bitan, T., Booth, J.R., Choy, J., Burman, D.D., Gitelman, D.R., Mesulam, M.M., 2005. Shifts of effective connectivity within a language network during rhyming and spelling. J. Neurosci. 25 (22), 5397–5403.
Canolty, R.T., Edwards, E., Dalal, S.S., Soltani, M., Nagarajan, S.S., Kirsch, H.E., Berger, M.S., Barbaro, N.M., Knight, R.T., 2006. High gamma power is phase-locked to theta oscillations in human neocortex. Science 313 (5793), 1626–1628.
Chawla, D., Lumer, E.D., Friston, K.J., 1999. The relationship between synchronization among neuronal populations and their mean activity levels. Neural Comput. 11 (6), 1389–1411 Aug 15.
Chen, C., Kiebel, S., Friston, K.J., 2008. Dynamic causal modelling of induced responses. NeuroImage 41, 1293–1312.
Darvas, F., Pantazis, D., Kucukaltun-Yildirim, E., Leahy, R.M., 2004. Mapping human brain function with MEG and EEG: methods and validation. NeuroImage 23 (Suppl. 1), S289–299.
David, O., Kiebel, S.J., Harrison, L.M., Mattout, J., Kilner, J.M., Friston, K.J., 2007. Dynamic causal modeling of evoked responses in EEG and MEG. NeuroImage 30 (4), 1255–1272.
Dayan, P., Hinton, G.E., Neal, R., Zemel, R.S., 1995. The Helmholtz Machine. Neural Comput. 7, 1022–1037.
Eaton, S.A., Salt, T.E., 1996. Role of N-methyl-D-aspartate and metabotropic glutamate receptors in corticothalamic excitatory postsynaptic potentials in vivo. Neuroscience 73, 1–5.
Ethofer, T., Anders, S., Erb, M., Herbert, C., Wiethoff, S., Kissler, J., Grodd, W., Wildgruber, D., 2006. Cerebral pathways in processing of affective prosody: a dynamic causal modeling study. NeuroImage 30 (2), 580–587.
Fairhall, S.L., Ishai, A., 2007. Effective connectivity within the distributed cortical network for face perception. Cereb. Cortex 17 (10), 2400–2406.
Felleman, D.J., Van Essen, D.C., 1991. Distributed hierarchical processing in the primate cerebral cortex. Cereb. Cortex 1, 1–47.

Faber, E.S., Sah, P., 2003. Calcium-activated potassium channels: multiple contributions to neuronal function. Neuroscientist 9, 181–194.
Fan, J., Hof, P.R., Guise, K.G., Fossella, J.A., Posner, M.I., 2008. The functional integration of the anterior cingulate cortex during conflict processing. Cereb. Cortex 18, 796–805.
Fox, K., Sato, H., Daw, N., 1989. The location and function of NMDA receptors in cat and kitten visual cortex. J. Neurosci. 9, 2443–2454.
Fox, K., Sato, H., Daw, N., 1990. The effect of varying stimulus intensity on NMDA receptor activity in cat visual cortex. J. Neurophysiol. 64, 1413–1428.
Friston, K.J., 2001. Brain function, nonlinear coupling, and neuronal transients. Neuroscientist 7 (5), 406–418.
Friston, K.J., 2003. Learning and inference in the brain. Neural Netw. 16, 1325–1352.
Friston, K., 2005. A theory of cortical responses. Philos. Trans. R. Soc. Lond., B Biol. Sci. 360 (1456), 815–836.
Friston, K.J., Ungerleider, L.G., Jezzard, P., Turner, R., 1995. Characterizing modulatory interactions between V1 and V2 in human cortex with fMRI. Hum. Brain Mapp. 2, 211–224.
Friston, K.J., Harrison, L., Penny, W., 2003. Dynamic causal modelling. NeuroImage 19, 1273–1302.
Friston, K., Kilner, J., Harrison, L., 2006. A free energy principle for the brain. J. Physiol. Paris 100 (1-3), 70–87.
Friston, K., Mattout, J., Trujillo-Barreto, N., Ashburner, J., Penny, W., 2007. Variational free energy and the Laplace approximation. NeuroImage 34 (1), 220–234.
Friston, K., Harrison, L., Daunizeau, J., Kiebel, S., Phillips, C., Trujillo-Barreto, N., Henson, R., Flandin, G., Mattout, J., 2008. Multiple sparse priors for the M/EEG inverse problem. NeuroImage 39 (3), 1104–1120.
Garrido, M.I., Kilner, J.M., Kiebel, S.J., Stephan, K.E., Friston, K.J., 2007. Dynamic causal modelling of evoked potentials: a reproducibility study. NeuroImage 36, 571–580.
Gentet, L.J., Ulrich, D., 2004. Electrophysiological characterization of synaptic connections between layer VI cortical cells and neurons of the nucleus reticularis thalami in juvenile rats. Eur. J. Neurosci. 19 (3), 625–633.
Girard, P., Bullier, J., 1989. Visual activity in area V2 during reversible inactivation of area 17 in the macaque monkey. J. Neurophysiol. 62, 1287–1301.
Grol, M.J., Majdandzić, J., Stephan, K.E., Verhagen, L., Dijkerman, H.C., Bekkering, H., Verstraten, F.A., Toni, I., 2007. Parieto-frontal connectivity during visually guided grasping. J. Neurosci. 27, 11877–11887.
Haxby, J.V., Hoffman, E.A., Gobbini, M.I., 2000. The distributed human neural system for face perception. Trends Cogn. Sci. 4, 223–233.
Helmholtz, H., 1860/1962. Handbuch der physiologischen optik. (English trans., Southall JPC, Ed.) Vol. 3. Dover, New York.
Henson, R.N., Goshen-Gottstein, Y., Ganel, T., Otten, L.J., Quayle, A., Rugg, M.D., 2003. Electrophysiological and haemodynamic correlates of face perception, recognition and priming. Cereb. Cortex 13, 793–805.
Henson, R.N., Mattout, J., Singh, K.D., Barnes, G.R., Hillebrand, A., Friston, K., 2007. Population-level inferences for distributed MEG source localization under multiple constraints: application to face-evoked fields. NeuroImage 38 (3), 422–438.
Hilgetag, C.C., O'Neill, M.A., Young, M.P., 2000. Hierarchical organisation of macaque and cat cortical sensory systems explored with a novel network processor. Philos. Trans. R. Soc. Lond., B Biol. Sci. 355, 71–89.
Hupe, J.M., James, A.C., Payne BR Lomber, S.G., Girard, P., Bullier, J., 1998. Cortical feedback improves discrimination between figure and background by V1, V2 and V3 neurons. Nature 394, 784–787.
Itier, R.J., Herdman, A.T., et al., 2006. Inversion and contrast-reversal effects on face processing assessed by MEG. Brain Res. 1115 (1), 108–120.
Jensen, O., Colgin, L.L., 2007. Cross-frequency coupling between neuronal oscillations. Trends Cogn. Sci. 11, 267–269.
Kawato M Hayakawa, H., Inui, T., 1993. A forward-inverse optics model of reciprocal connections between visual cortical areas. Network 4, 415–422.
Kelly, J.B., Zhang, H., 2002. Contribution of AMPA and NMDA receptors to excitatory responses in the inferior colliculus. Hear. Res. 168, 35–42.
Kersten, D., Mamassian, P., Yuille, A., 2004. Object perception as Bayesian inference. Annu. Rev. Psychol. 55, 271–304.
Kiebel, S.J., Daunizeau, J., Phillips, C., Friston, K.J., 2008. Variational Bayesian inversion of the equivalent current dipole model in EEG/MEG. NeuroImage 39 (2), 728–741.
Kilner, J.M., Mattout, J., Henson, R., Friston, K.J., 2005. Hemodynamic correlates of EEG: a heuristic. NeuroImage 28, 280–286.
Klopp, J., Halgren, E., Marinkovic, K., Nenov, V., 1999. Face-selective spectral changes in the human fusiform gyrus. Clin. Neurophysiol. 110, 676–682.
Klopp, J., Marinkovic, K., Chauvel, P., Nenov, V., Halgren, E., 2000. Early widespread cortical distribution of coherent fusiform face selective activity. Hum. Brain Mapp. 11, 286–293.
Lamme, V.A., Roelfsema, P.R., 2000. The distinct modes of vision offered by feedforward and recurrent processing. Trends Neurosci. 23 (11), 571–579.
Lamme, V.A., Supèr, H., Spekreijse, H., 1998. Feedforward, horizontal, and feedback processing in the visual cortex. Curr. Opin. Neurobiol. 8 (4), 529–535.
Larkum, M.E., Senn, W., Luscher, H.R., 2004. Top-down dendritic input increases the gain of layer 5 pyramidal neurons. Cereb. Cortex 14, 1059–1070.
London, M., Häusser, M., 2005. Dendritic computation. Annu. Rev. Neurosci. 28, 503–532.
MacKay, D.M., 1956. The epistemological problem for automata. In: Shannon, CE, McCarthy, J (Eds.), Automata Studies. Princeton University Press, Princeton, NJ, pp. 235–251.
Maunsell, J.H., van Essen, D.C., 1983. The connections of the middle temporal visual area (MT) and their relationship to a cortical hierarchy in the macaque monkey. J. Neurosci. 3, 2563–2586.
Mechelli, A., Price, C.J., Noppeney, U., Friston, K.J., 2003. A dynamic causal modeling study on category effects: bottom-up or top-down mediation? J. Cogn. Neurosci. 15 (7), 925–934.
Metherate, R., Cox, C.L., Ashe, J.H., 1992. Cellular bases of neocortical activation: modulation of neural oscillations by the nucleus basalis and endogenous acetylcholine. J. Neurosci. 12, 4701–4711.
Michel, C.M., Murray, M.M., Lantz, G., Gonzalez, S., Spinelli, L., Grave de Peralta, R., 2004. EEG source imaging. Clin. Neurophysiol. 115, 2195–2222.
Moran, R.J., Stephan, K.E., Kiebel, S.J., Rombach, N., O'Connor, W.T., Murphy, K.J., Reilly, R.B., Friston, K., 2008. Bayesian estimation of synaptic physiology from the spectral responses of neural masses. NeuroImage 42, 272–284.
Mumford, D., 1992. On the computational architecture of the neocortex. II. The. role. of. cortico-cortical. loops. Biol. Cybern. 66, 241–251.
Murphy, P.C., Sillito, A.M., 1987. Corticofugal feedback influences the generation of length tuning in the visual pathway. Nature 329, 727–729.
Penny, W.D., Stephan, K.E., Mechelli, A., Friston, K.J., 2004. Comparing dynamic causal models. NeuroImage 22, 1157–1172.
Rao, R.P., 1999. An optimal estimation approach to visual perception and learning. Vis. Res. 39, 1963–1989.
Rao, R.P., Ballard, D.H., 1999. Predictive coding in the visual cortex: a functional interpretation of some extra-classical receptive field effects. Nat. Neurosci. 2, 79–87.
Rivadulla, C., Martinez, L.M., Varela, C., Cudeiro, J., 2002. Completing the corticofugal loop: a visual role for the corticogeniculate type 1 metabotropic glutamate receptor. J. Neurosci. 22, 2956–2962.
Rockland, K.S., Pandya, D.N., 1979. Laminar origins and terminations of cortical connections of the occipital lobe in the rhesus monkey. Brain Res. 179, 3–20.
Rosier, A.M., Arckens, L., Orban, G.A., Vandesande, F., 1993. Laminar distribution of NMDA receptors in cat and monkey visual cortex visualized by [3H]-MK-801 binding. J. Comp. Neurol. 335, 369–380.
Rossion, B., Caldara, R., Seghier, M., Schuller, A.M., Lazeyras, F., Mayer, E., 2003. A network of occipito-temporal face-sensitive areas besides the right middle fusiform gyrus is necessary for normal face processing. Brain 126, 2381–2395.
Salin, P.A., Bullier, J., 1995. Corticocortical connections in the visual system: structure and function. Psychol. Bull. 75, 107–154.
Salt, T.E., 2002. Glutamate receptor functions in sensory relay in the thalamus. Philos. Trans. R. Soc. Lond., B Biol. Sci. 357, 1759–1766.
Sandell, J.H., Schiller, P.H., 1982. Effect of cooling area 18 on striate cortex cells in the squirrel monkey. J. Neurophysiol. 48, 38–48.
Schiller, J., Schiller, Y., 2001. NMDA receptor-mediated dendritic spikes and coincident signal amplification. Curr. Opin. Neurobiol. 11 (3), 343–348.
Sherman, S.M., Guillery, R.W., 1998. On the actions that one nerve cell can have on another: distinguishing "drivers" from "modulators". Proc. Natl. Acad. Sci. U. S. A. 95, 7121–7126.
Shipp, S., 2005. The importance of being agranular: a comparative account of visual and motor cortex. Philos. Trans. R. Soc. Lond., B Biol. Sci. 360 (1456), 797–814.
Singh, K.D., Barnes, G.R., Hillebrand, A., 2003. Group imaging of task-related changes in cortical synchronisation using nonparametric permutation testing. NeuroImage 19, 1589–1601.
Soltesz, I., Deschênes, M., 1993. Low- and high-frequency membrane potential oscillations during theta activity in CA1 and CA3 pyramidal neurons of the rat hippocampus under ketamine-xylazine anesthesia. J. Neurophysiol. 70 (1), 97–116.
Stephan, K.E., Marshall, J.C., Penny, W.D., Friston, K.J., Fink, G.R., 2007a. Interhemispheric integration of visual processing during task-driven lateralization. J. Neurosci. 27, 3512–3522.
Stephan, K.E., Weiskopf, N., Drysdale, P.M., Robinson, P.A., Friston, K.J., 2007b. Comparing hemodynamic models with DCM. NeuroImage 38, 387–401.
Stephan, K.E., Kasper, L., Harrison, L.M., Daunizeau, J., den Ouden, H.E., Breakspear, M., Friston, K.J., 2008. Nonlinear dynamic causal models for fMRI. Neuroimage 42, 649–662.
Summerfield, C., Egner, T., Greene, M., Koechlin, E., Mangels, J., Hirsch, J., 2006. Predictive codes for forthcoming perception in the frontal cortex. Science 314, 1311–1314.
Talairach, J., Tournoux, P., 1988. Co-planar Stereotaxic Atlas of the Human Brain: 3-Dimensional Proportional System - an Approach to Cerebral Imaging. Thieme Medical Publishers, New York, NY.
Tallon-Baudry, C., Bertrand, O., 1999. Oscillatory gamma activity in humans and its role in object representation. Trends Cogn. Sci;. 3, 151–162.
Varela, F., Lachaux, J.P., Rodriguez, E., Martinerie, J., 2001. The brainweb: phase synchronization and large-scale integration. Nat. Rev., Neurosci. 2, 229–239.
Winston, J.S., Henson, R.N., Fine-Goulden, M.R., Dolan, R.J., 2004. fMRI-adaptation reveals dissociable neural representations of identity and expression in face perception. J. Neurophysiol. 92, 1830–1839 2004.
Zeki, S., Shipp, S., 1988. The functional logic of cortical connections. Nature 335, 311–317.